JOURNAL OF MARITIME RESEARCH

Vol XXII. No. II (2025) pp 220–227

ISSN: 1697-4840, www.jmr.unican.es

Hydrodynamic Interaction Coefficients for an Array of Freely Floating Bodies in Waves

Mir Tareque Ali[1,*], Kazi Naimul Hoque[2]

ARTICLE INFO

Article history:
Received 02 Oct 2024;
in revised from 10 Oct 2024;
accepted 15 Nov 2024.

Keywords:
Hydrodynamic interaction, Multi-body, Added mass, Damping coefficient, Frequency domain.

ABSTRACT

This paper examines the hydrodynamic interaction coefficients for added mass and damping of multiple arbitrarily shaped three-dimensional (3-D) bodies floating freely in close proximity to one another. Numerical simulations were performed using Hydrostar, a commercial hydrodynamic software developed by Bureau Veritas. Initially, the simulations were carried out for a box-cylinder model and a modified Wigley-rectangular barge model. The simulation results for the hydrodynamic interaction coefficients were validated by comparing them with published results and the agreement was found quite satisfactory. Subsequent simulations were conducted for an array of identical truncated composite circular cylinders floating vertically in regular waves, positioned close to each other. During the computation of the hydrodynamic interaction coefficients for this multi-body configuration, both the number of cylinders in the array and the gap width between them were varied. The study also investigated the occurrence of hydrodynamic resonances in the gaps between the floating bodies and the presence of sharp spikes in the results of the diagonal and cross-coupling interaction terms. Finally, some conclusions were drawn based on the findings of the analysis.

1. Introduction.

In offshore engineering, numerous applications involve two or more floating structures operating in close proximity within harsh ocean environments. Examples include very large floating structures, mobile offshore drilling units, floating bridges, arrays of floating offshore renewable energy platforms, offshore float-over installations, floating platforms supported by multiple vertical columns, and loading/offloading operations for LNG-FPSO systems.

In fact, when multiple floating bodies are positioned close together in waves, each body is affected by interactions caused by the presence of nearby structures. Additionally, the gaps between them influence wave forces and the motion responses of the bodies. To ensure the safety and optimal performance of such a multi-body floating system, it is essential to investigate the characteristics of the hydrodynamic interaction coefficients of these structures.

The hydrodynamic interactions between multiple floating bodies have been reported by many researchers. Oortmerssen [1] used the 3-D linear diffraction theory to solve hydrodynamic interaction problem for multiple floating bodies. Goo and Yoshida [2] used combined source distribution method and an interaction theory for predicting the wave forces on multiple 3-D bodies of arbitrary shape freely floating in waves and the resultant motion response of the multiple bodies. Inoue and Ali [3] applied 3-D source distribution technique to compute motion responses and drift forces for multiple floating bodies in frequency domain and time domain simulations. Hong et al. [4] used a higher-order boundary element method (HOBEM) to predict motion and drift force of side-by-side moored LNG FPSO and LNGC. Molin et al. [5] carried out model tests

[1]Professor, Department of Naval Architecture & Marine Engineering, Bangladesh University of Engineering & Technology, Dhaka-1000, Bangladesh.

[2]Assistant Professor, Department of Naval Architecture & Marine Engineering, Bangladesh University of Engineering & Technology, Dhaka-1000, Bangladesh.

[*]Corresponding author: Mir Tareque Ali. E-mail Address: mtarequeali@name.buet.ac.bd.

with two side-by-side rectangular barge models and measured the free surface elevations at different locations along the gap. Sayeed [6] conducted both experimental and numerical investigation to study the hydrodynamic effects on small ice masses. Ghafari et al. [7] studied the hydrodynamic interactions in frequency domain and time domain for Amirkabir semi-submersible and a Mono column FPSO floating platform in Caspian Sea Conditions. Fenerci et al. [8] examined the hydrodynamic interaction effects among the pontoons of a floating bridge. Liu et al. [9] utilized the Reynolds-averaged Navier-Stokes (RANS) method, and the hydrodynamic interference between two KRISO Container Ships (KCS) operating in still water was investigated.

This paper investigates the hydrodynamic interaction coefficients for added mass and damping of multiple arbitrarily shaped 3-D bodies floating freely in close proximity to one another. Numerical simulations were performed using Hydrostar, a commercial hydrodynamic software developed by Bureau Veritas. Initially, the simulations were carried out for a box-cylinder model and a modified Wigley-rectangular barge model. The simulation results for the hydrodynamic interaction coefficients were validated against the published results and the agreement was found quite satisfactory. Subsequent simulations were conducted for an array of identical truncated composite circular cylinders floating vertically in regular waves, positioned close to each other. During the simulations of this configuration, both the number of cylinders in the array and the gap width between them were varied. The study also investigated the occurrence of hydrodynamic resonances in the gaps between the floating bodies and the presence of sharp spikes in the results of the diagonal and cross-coupling interaction terms.

2. Mathematical Formulation of the Problem.

2.1. Assumptions and coordinate systems.

Consider an array of 'm' number of 3-D bodies of arbitrary shape, oscillating sinusoidally in close proximity with the waves in water of uniform depth. The amplitudes of the motions of the bodies and waves are assumed to be small, whereas the fluid is supposed to be homogeneous, incompressible, inviscid and the flow is irrotational. Two coordinate systems, a global coordinate system $(O_0 - X_0Y_0Z_0)$ which is fixed in space and local coordinate systems $(O_1 - X_1Y_1Z_1), (O_2 - X_2Y_2Z_2) \ldots\ldots\ldots$-$(O_m - X_mY_mZ_m)$ which are fixed with respect to the mean position of each body floating freely close to each other, is shown in Fig. 1. The origin of each coordinate system is placed on a calm water surface and the z-axis is positive vertically in the upward direction.

2.2. Velocity Potentials.

In regular waves a linear potential $\emptyset$, which is a function of space and of time, can be written as a product of space-dependent term and a harmonic time-dependent term as follows:

$$\emptyset(x, y, z; t) = Re[\varphi(x, y, z).e^{-i\omega t}] \tag{1}$$

Figure 1: Definition of coordinate system for multiple floating bodies in waves.

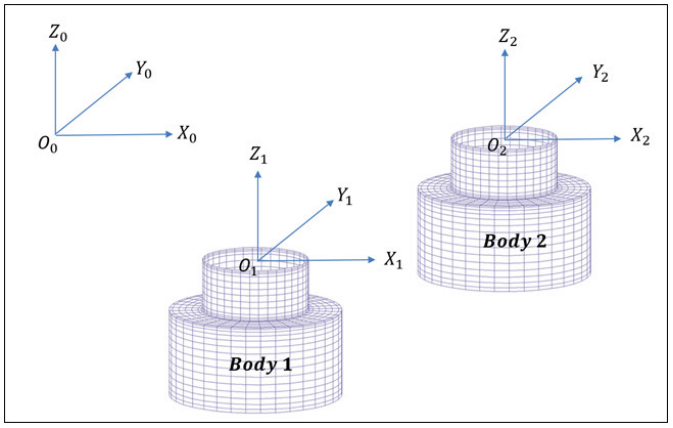

Source: Authors.

where $\varphi(x, y, z)$ is time independent quantity and the potential function $\varphi(x, y, z)$ can be separated into contributions from all modes of motion of the bodies and from the incident and diffracted wave fields as follows:

$$\varphi = -i\omega\left[(\varphi_0 + \varphi_7)\,\zeta_a + \sum_{j=1}^{6}\eta_j^1\varphi_j^1 + \cdots + \sum_{j=1}^{6}\eta_j^m\varphi_j^m\right] \tag{2}$$

where φ_0 is the incident wave potential, φ_7 is the diffraction wave potential, φ_j^1 represent potentials due to motion of body 1 in the j-th mode, φ_j^m represent potentials due to motion of body m in the j-th mode i.e., radiation wave potentials, η_j^1 is the motion of body 1 in j-th mode, η_j^m is the motion of body m in j-th mode and ζ_a is the incident wave amplitude. The incident wave potential can be expressed as:

$$\varphi_0 = \frac{g}{\omega^2}\frac{\cosh[k\,(z+h)]}{\cosh kh}e^{ik(x\cos\beta + y\sin\beta)} \tag{3}$$

where β is the angle of incident wave relative to the positive x-axis, h is the depth of water, g is the acceleration due to gravity and k is the wave number. The individual potentials are the solutions of Laplace equation and they need to satisfy the boundary conditions. According to the 3-D source distribution method, the potentials φ_7 and φ_j^m can be expressed in terms of well-known Green functions and as a result, boundary conditions are reduced to only on the wetted surfaces of the bodies [12].

2.3. Source density and Green's function.

The potential function at some point (x, y, z) in the fluid region in terms of source distribution can be written as:

$$\varphi_j^m(x, y, z) = \frac{1}{4\pi}\iint_{S_B^m}\sigma^m(\xi, \eta, \zeta)\,G(x, y, z; \xi, \eta, \zeta)\,dS \qquad j = (1, 2, 3, \ldots, 7) \tag{4}$$

where $G(x, y, z; \xi, \eta, \zeta)$ denotes the Green's function of a source, singular in (ξ, η, ζ) and $\sigma_j^m(\xi, \eta, \zeta)$ is the complex source strength. Since Green's function satisfies the boundary conditions, applying the kinematics boundary condition on the immersed surface yields the following integral equation:

$$\frac{\partial \varphi_j^m(x,y,z)}{\partial n} = -\frac{1}{2}\sigma_j^m(x,y,z) + \frac{1}{4\pi}\iint_{S_B^m} \sigma_j^m(\xi,\eta,\zeta)\frac{\partial}{\partial n}G(x,y,z;\xi,\eta,\zeta)\,dS \qquad (5)$$
$$j = (1, 2, 3, \ldots, 7)$$

2.4. Hydrodynamic Interaction Coefficients.

Based on the linearized Bernoulli's equation, the hydrodynamic pressure distribution can be calculated by the following equation,

$$p = -\rho\frac{\partial \Phi}{\partial t} = \rho\omega^2\left[(\varphi_0 + \varphi_7)\zeta_\alpha + \sum_{j=1}^{6}\eta_j^1\varphi_j^1 + \ldots + \sum_{j=1}^{6}\eta_j^m\varphi_j^m\right]e^{-i\omega t} \qquad (6)$$

Hydrodynamic reactive forces in the k-th mode on body 'm' can be written as follows:

$$F_k^m = -\rho\omega^2 e^{-i\omega t}\sum_{j=1}^{6}\iint_{S^m}\left[\varphi_j^1\eta_j^1 + \ldots \varphi_j^m\eta_j^m\right]n_k^m\,dS \qquad (7)$$

The reactive forces can be thought of having one component in phase with the body acceleration and another in phase with body velocity as follows:

$$F_k = -\left(a_{kj}\ddot{\eta}_j + b_{kj}\dot{\eta}_j\right) = \left(\omega^2 a_{kj} + i\omega b_{kj}\right)\eta_j e^{-i\omega t} \qquad (8)$$

Upon equating the real and imaginary parts of equations (7) and (8), the added mass and damping coefficients due to own body motion and due to other body motion i.e., interaction coefficients can be written as presented in Table 1:

Table 1: Hydrodynamic Interaction Coefficients.

Added mass coefficient	Damping coefficient
$a_{kj}^{mn} = -Re\left[\rho\iint_{S^m}\varphi_j^n n_k^m dS\right]$	$b_{kj}^{mn} = -Im\left[\rho\omega\iint_{S^m}\varphi_j^n n_k^m dS\right]$
$a_{kj}^{nm} = -Re\left[\rho\iint_{S^n}\varphi_j^m n_k^n dS\right]$	$b_{kj}^{nm} = -Im\left[\rho\omega\iint_{S^n}\varphi_j^m n_k^n dS\right]$

Source: Authors.

where a_{kj}^{mn} and b_{kj}^{mn} are the added-mass and damping coefficient respectively in the k-th direction of m-th body due to j-th mode of motion of n-th body.

According to Dmitrieva [10], for multi-body motions the hydrodynamic interaction coefficients satisfy the symmetry relationships, i.e.,

$$a_{kj}^{mn} = a_{jk}^{nm} \qquad (9)$$

$$b_{kj}^{mn} = b_{jk}^{nm} \qquad (10)$$

3. Results and Discussions.

Numerical simulations were performed using Hydrostar, a commercial hydrodynamic software developed by Bureau Veritas. Initially, the simulations were carried out for a box-cylinder model and a modified Wigley-rectangular barge model. The simulation results for the hydrodynamic interaction coefficients were validated by comparing them with published results and the agreement was found quite satisfactory. Subsequent simulations were conducted for an array of identical truncated composite circular cylinders floating vertically in regular waves, positioned close to each other. During the simulations for this configuration of multi-bodies, both the number of cylinders in the array and the gap width between them were varied. The study also investigated the occurrence of hydrodynamic resonances in the gaps between the floating bodies and the presence of sharp spikes in the results of the diagonal and cross-coupling interaction terms.

3.1. Rectangular Box and Vertical Cylinder Model.

To study the characteristics of hydrodynamic interaction coefficients for multiple floating bodies, numerical computation is initially carried out for a vertical cylinder (body 1) and a rectangular box (body 2) model freely floating in close proximity in regular waves [10]. The vertical cylinder is 95.8 m in diameter and 30.0 m in draft, whereas the rectangular box is 109.7 m in length, 101.4 m in breadth and 30 m in draft. The wetted surfaces of the vertical cylinder (body 1) and the rectangular box (body 2) are divided into 1034 and 2240 panels respectively. The 3-D mesh arrangements and the plan view of the box-cylinder model in side-by-side configuration are presented in Fig. 2(a) and 2(b) respectively.

Numerical simulations are conducted for the gap width of 50.0 m between the two bodies floating in water of 220 m in depth. The hydrodynamic interaction coefficients of added mass and damping for surge and heave are non-dimensionalized by dividing with $\rho\zeta_a\nabla$ and $\rho\zeta_a\nabla\sqrt{g/l}$ respectively and the wave frequency is non-dimensionalized by multiplying with $\sqrt{l/g}$, where the characteristics length l is 101.4 m.

Figs. 3(a) and 3(b) show the results of diagonal terms (surge-surge) of non-dimensional hydrodynamic interaction coefficients for added mass ${}^{11}a_{11}^*$ and ${}^{22}a_{11}^*$ of the body 1 (cylinder) and body 2 (box) due to their own motion for surge mode. Figs. 4(a) and 4(b) on the other hand, present the results of cross-coupling (surge-heave) non-dimensional hydrodynamic interaction coefficients for added mass ${}^{21}a_{31}^*$ and ${}^{12}a_{13}^*$ damping ${}^{21}b_{31}^*$ and ${}^{12}b_{13}^*$of body 1 (cylinder) and body 2 (box) due to the motion of other bodies and vice versa. The present numerical results

Figure 2: (a) 3-D view of mesh arrangements and (b) Plan view for box and cylinder model.

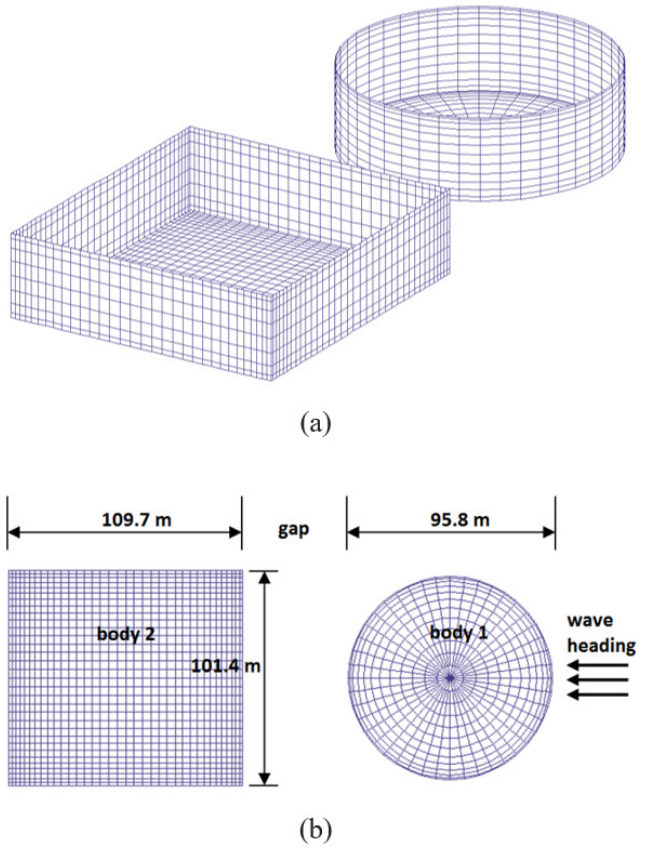

Source: Authors.

Figure 3: Hydrodynamic interaction coefficients for floating box and cylinder model.

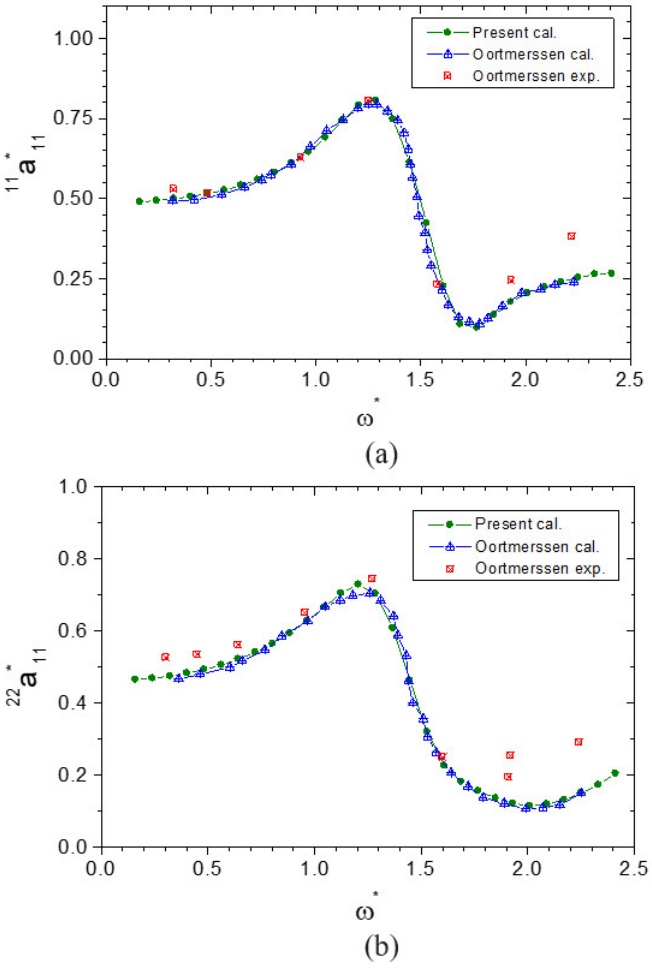

Source: Authors.

are compared with the numerical and experimental results of Oortmerssen [10]. As can be seen from these figures, that the agreement between the calculated results are quite satisfactory, however the agreement with the experimental results present some deviations. Moreover, figures 4(a) and 4(b) demonstrate that the symmetry relationships exist for hydrodynamic interaction coefficients.

3.2. *Modified Wigley and rectangular barge model.*

The second multi-body problem selected for the present study is a modified Wigley (Ship-A) and a rectangular barge model (Ship-B) [11]. The principal dimensions of these floating bodies are presented in Table 2. For numerical simulations, the wetted surfaces of Ship-A and Ship-B are divided into 480 and 608 panels respectively, as shown in Fig. 5. During the simulations of this configuration, the water depth is taken as 7.00 m. Figs. 6(a) and 6(b), present the hydrodynamic interaction coefficients for added mass and damping for this model when the separation distance between them is 1.797m. The present numerical results are compared with the numerical and experimental results of Kashiwagi et al. [11]. As can be seen from these figures, that the agreement between the present and published results are quite satisfactory.

3.3. *Array of Truncated Composite Cylinders.*

The third multi-body model selected for the present study is an array of identical truncated composite circular cylinders freely floating vertically close to each other in regular waves. The wetted surfaces for each of the composite cylinders are divided into 1566 panels and the 3-D view of the mesh arrangements of an isolated cylinder is shown in Fig. 7. The top diameter, base diameter and total draft of each cylinder are 16.5 m, 27.0 m and 21.5 m respectively. The center of gravity of each cylinder is considered at 15m below the free water surface and the depth of water is 100m. The schematic view of an array of equally-spaced 5 identical cylinders (5body case) is shown in Fig. 8, where the center to center distances between adjoining cylinders are 54m. For numerical simulations, four different cases namely 1body (body 1 only), 2body (body1 and body2 only), 3body (body1, body2 and body3 only) and 5body (body1, body2, body3, body4 and body5) are considered. The gap width between these equally-spaced cylinders is varied as 27 m, 54 m and 81 m.

Figure 4: Hydrodynamic interaction coefficients for floating box and cylinder model.

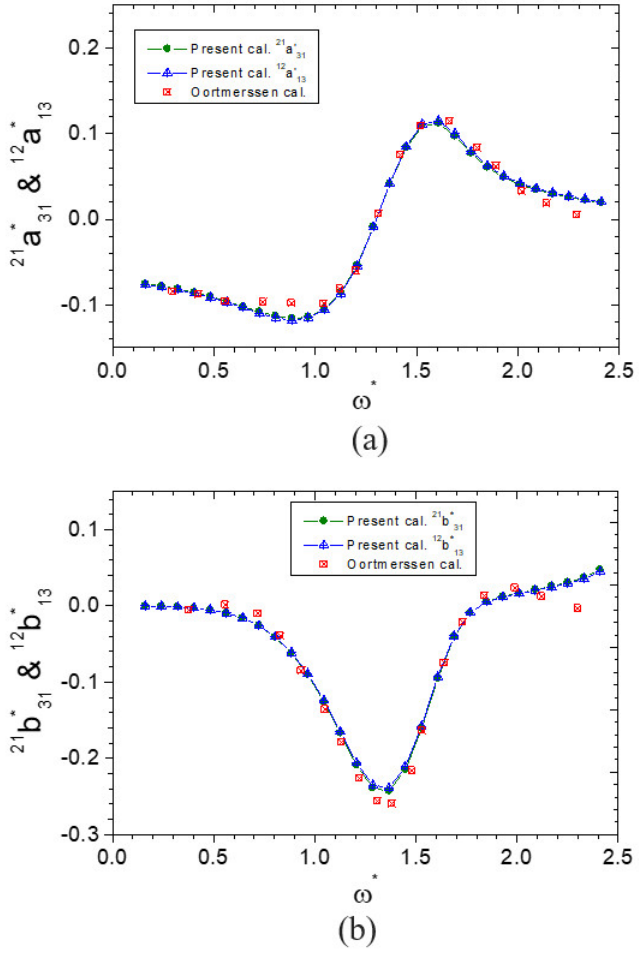

Source: Authors.

Table 2: Principal dimensions of Wigley-barge model.

Parameters	Modified wigley model	Rectangular barge
Length	2.00 m	2.00 m
Breadth	0.30 m	0.30 m
Draught	0.125 m	0.125 m
Waterplane area	0.416 m^2	0.600 m^2
Displacement	0.04205 m^3	0.075 m^3

Source: Authors.

The non-dimensional hydrodynamic interaction coefficients are shown in Table 3 and the numerical results are presented against non-dimensional wave frequency ($\omega^* = \omega\sqrt{l/g}$), where the characteristics length, l = 27.0 m. Figures 9(a)-9(f) show the results of diagonal terms (11, 33 and 55) for surge, heave and pitch mode of non-dimensional hydrodynamic interaction coefficients of added mass and damping. And the figures display only body1 results for 1body, 2body, 3body and 5body cases for a fixed gap of 27m between adjoining cylinders. It is clearly evident from these figures that hydrodynamic interactions become more and more prominent as the number of bodies in the array is gradually increased. The interaction effects are almost absent (weak) for lower frequency range ($\omega^* \leq 1.0$).

Figure 5: 3-D view of mesh arrangements for a modified Wigley and rectangular barge model.

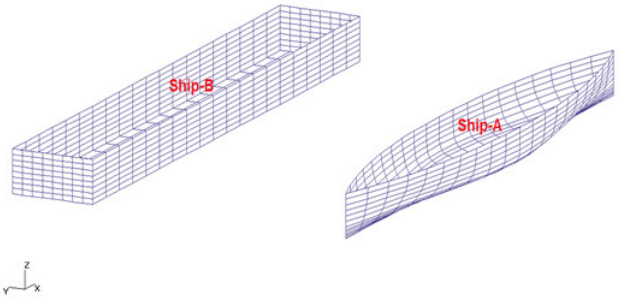

Source: Authors.

Figure 6: Hydrodynamic interaction coefficients for a modified Wigley and rectangular barge model.

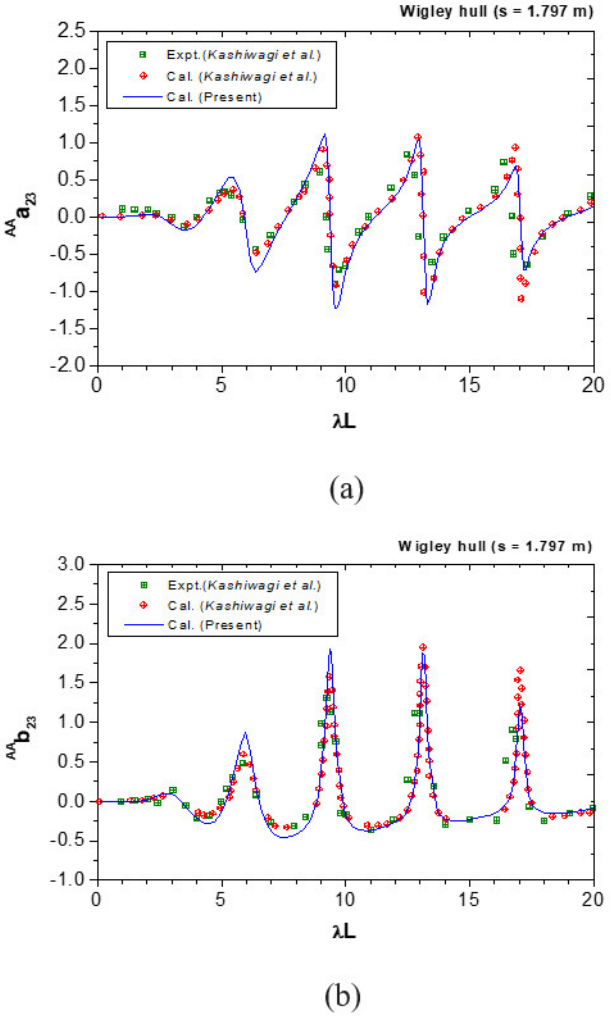

Source: Authors.

Figure 7: 3-D view of the mesh arrangement of an isolated composite cylinder.

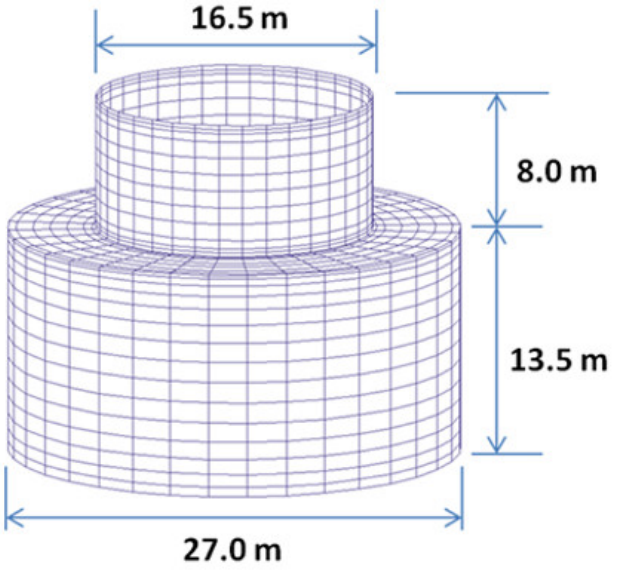

Source: Authors.

Table 3: Definition of non-dimensional hydrodynamic interaction coefficients.

Added mass	Damping	Mode
$a^*_{kj} = \frac{a_{kj}}{\rho\zeta_a\nabla}$	$b^*_{kj} = \frac{b_{kj}}{\rho\zeta_a\nabla\sqrt{g/l}}$	$k = j = 1$ $k = j = 3$ $k = 1, j = 3$
$a^*_{kj} = \frac{a_{kj}}{\rho\zeta_a\nabla l^2}$	$b^*_{kj} = \frac{b_{kj}}{\rho\zeta_a\nabla l^2\sqrt{g/l}}$	$k = j = 5$
$a^*_{kj} = \frac{a_{kj}}{\rho\zeta_a\nabla l}$	$b^*_{kj} = \frac{b_{kj}}{\rho\zeta_a\nabla l\sqrt{g/l}}$	$k = 1, j = 5$ $k = 3, j = 5$

Source: Authors.

For surge added mass and damping results, i.e., Figs. 9(a) and 9(b), strong interaction is observed with spikes and rapid fluctuation within a frequency range of ($1.0 \leq \omega^* \leq 2.5$). On the other hand, interaction effect is weak for heave mode as displayed in Figs. 9(c) and 9(d). For pitch added mass and damping results, i.e., Figs. 9(e) and 9(f), strong interaction is observed with spikes and fluctuations for higher frequency range ($\omega^* > 1.0$). Moreover, a noticeable sharp spike appears for surge and pitch damping at $\omega^* = 1.65$, which may be attributed due to resonance of water within the gap.

Figures 10(a)-10(f) also present the results of diagonal terms (11, 33 and 55) for surge, heave and pitch mode of non - dimensional hydrodynamic interaction coefficients of added mass and damping. In this case, the figures give only body1 results due to its own motion within an array of 5 bodies (5body case) for the gap widths of 27m, 54m and 81m between adjoining cylinders.

Figure 8: The schematic view of an array of equally-spaced 5 identical cylinders (5body case).

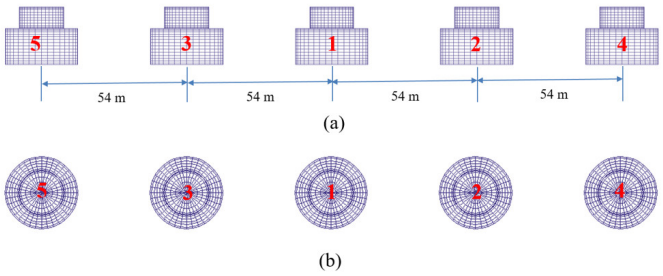

Source: Authors.

Figure 9: Hydrodynamic interaction coefficients for array of identical freely floating circular cylinders for surge, heave and pitch mode.

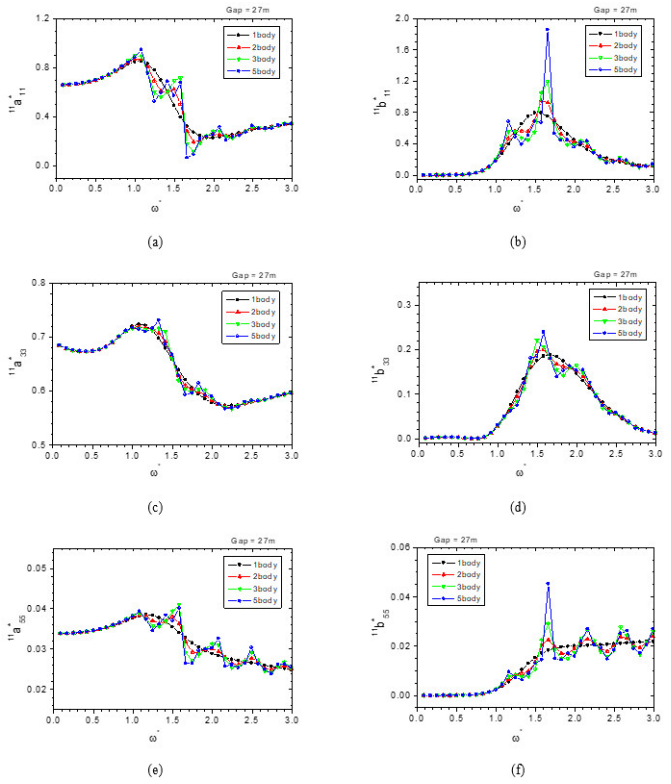

Source: Authors.

It is evident from these figures that strong hydrodynamic interactions occur as the gap width is reduced in the array. Similar to the previous results, the interaction effects in this case are also almost absent (weak) for lower frequency range ($\omega^* \leq 1.0$). For surge added mass and damping results, i.e., Figs. 10(a) and 10(b), strong interaction is observed with spikes and rapid fluctuation within a frequency range of ($1.0 \leq \omega^* \leq 2.5$). On the other hand, interaction effect is weak for heave mode as displayed in Figs. 10(c) and 10(d). For pitch added mass and damping results, i.e., Figs. 10(e) and 10(f), strong interaction is observed with spikes and fluctuations for higher frequency range ($\omega^* > 1.0$). Similar to Figs 9(b) and 9(f), noticeable

sharp spike appears for surge and pitch damping at $\omega^* = 1.65$.

Figure 10: Hydrodynamic interaction coefficients for an array of identical freely floating circular cylinders for surge, heave and pitch mode.

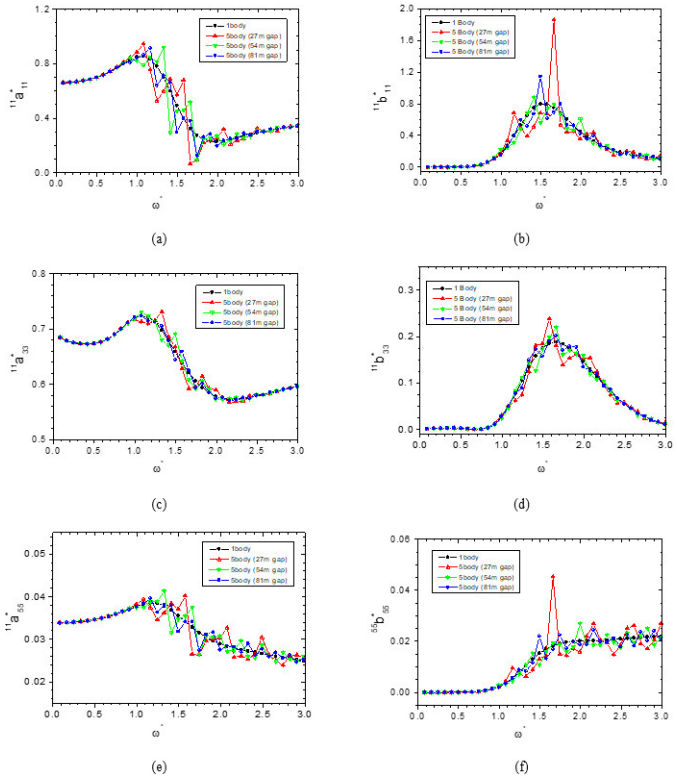

Source: Authors.

Figs. 11(a)- 11(f) display the cross-coupling term (13, 35 and 15) results of hydrodynamic interaction coefficients. The gap width between the array members is fixed at 27m for 2body, 3body and 5body cases. Unlike the results for diagonal terms, the cross-coupling term results are not affected significantly as the numbers of cylinders are increased in the array. Moreover, the numerical results clearly exhibit that the symmetry relationships exist for hydrodynamic interaction coefficients.

Observing the numerical results presented in Figs. 9, 10 and 11, one can find some characteristics trends for hydrodynamic interaction coefficients among the members in the array of floating cylinders. Spikes and rapid fluctuations are present in most of the curves while comparing to that of an isolated cylinder (1 body) results. One of the probable reasons might be the presence of surrounding bodies as well as their sheltering effect on body1 within the array for which most of the results are presented. The other reason might be the existence of piston mode and sloshing modes of the water body in-between the floating cylinders [5]. The oscillating local peaks in the coefficients at certain frequencies indicate resonances occurring between the members in the array. And the numerical computations show that the non-dimensional resonance wave frequencies (ω^*) appears around $\sqrt{n\pi}$ *where*, $(n = 1, 2, \ldots, \infty)$ with a corresponding frequency shift for different array configurations [5]. Using this simplified formulations the estimated lowest two mode of non-dimensional resonance frequencies (ω^*) are found as 1.77 and 2.50 for $n = 1$ *and* $n = 2$ respectively. Using the simplified formulations of Thus, the location of resonance frequencies and the characteristics of numerical results for hydrodynamic interaction coefficients will depend on the complex geometry of the composite cylinders as well as the gap in between these floating bodies.

Figure 11: Hydrodynamic interaction coefficients for an array of identical freely floating circular cylinders for surge, heave and pitch mode.

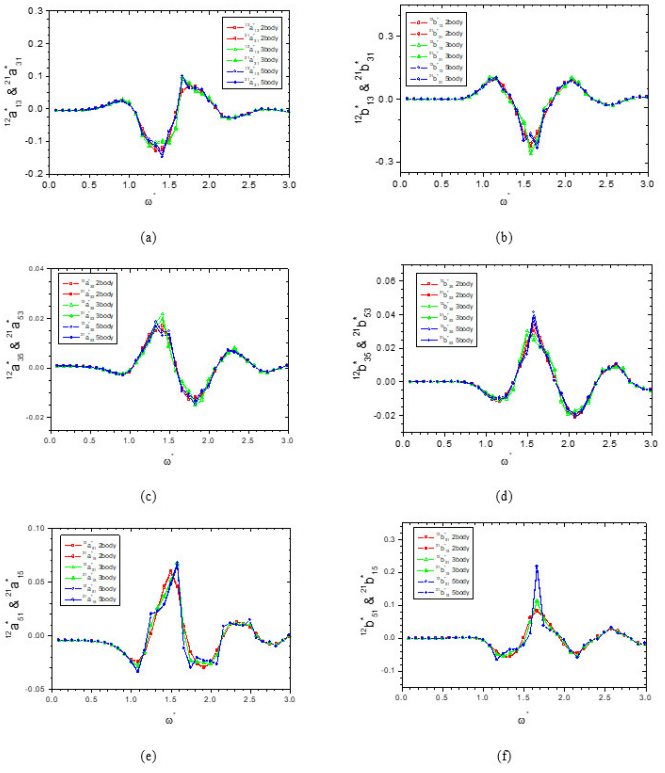

Source: Authors.

Conclusions.

Based on the 3-D source distribution method, a commercial hydrodynamic software, Hydrostar has been adopted to study the hydrodynamic interaction coefficients of added mass and damping for an array of identical truncated composite circular cylinders freely floating vertically close to each other in regular waves. Hydrodynamic interaction effects are very weak at lower frequency range ($\omega^* \leq 1.0$). For a fixed gap width, hydrodynamic interactions become more and more prominent as the number of bodies in the array is gradually increased. For a particular array of floating bodies, as the gap widths between the members are gradually decreased, spikes with higher magnitude appear in the numerical results. As the number of bodies in the group is increased the influence of hydrodynamic interaction coefficients for diagonal terms are affected significantly, however for cross-coupling terms the influence is very

weak. Resonance phenomenon may be attributed for the presence of sharp spikes in the computed results. The symmetry relationship exists for the hydrodynamic interaction coefficients of added mass and damping for floating multi-body problem.

References.

[1] Van Oortmerssen, G., 1979, "Hydrodynamic Interaction between Two Structures of floating in Waves," Proc. 2nd Int'l Conf. of Behavior of Offshore Structures, BOSS, London, pp.339-356.

[2] Goo, J. and Yoshida, K., 1989, "Hydrodynamic interaction between multiple three dimensional bodies of arbitrary shape in waves," Journal of the Society of Naval Architects of Japan, Vol. 165, pp. 193-202. http://worldcat.org/issn/05148499.

[3] Inoue, Y. and Ali, M. T., 2002, "A study on numerical accuracy for the prediction of motion responses and drift forces of multiple floating bodies," Journal of the Society of Naval Architects of Japan, Vol. 192, pp. 289-298. https://doi.org/10.2534/jjasnaoe1968.2002.289.

[4] Hong, S. Y., Kim, J. H., Cho, S. K., Choi, Y. R., Kim, Y. S., 2005, "Numerical and Experimental Study on Hydrodynamic Interaction of Side-by-Side Moored Multiple Vessels, " Ocean Engineering, 32, pp. 783-801. https://doi.org/10.1016/j-.oceaneng.2004.10.003.

[5] Molin, B., Remy, F., Camhi, A., Ledoux, A., 2009, "Experimental and numerical study of the gap resonances inbetween two rectangular barges, " 13th Congress of International Maritime Association of Mediterranean IMAM 2009, Istambul, Turkey. https://hal.science/hal-00454571.

[6] Sayeed, T. M., 2017, "Hydrodynamic interaction of wave driven icebergs in close proximity with a fixed offshore structure, " Ph. D. Thesis, Faculty of Engineering and Applied Science, Memorial University of Newfoundland.

[7] Ghafari, H., Ketabdari, M., Ghassemi, H. and Homayoun, E., 2019, "Numerical Study on the Hydrodynamic Interaction between two Floating Platforms in Caspian Sea Environmental Conditions," Ocean Engineering, 188. https://doi.org/10.1016/j.oceaneng.2019.106273.

[8] Fenerci, A., Kvåle, K. A., Xiang, Xu., and Øiseth, O., 2022, "Hydrodynamic interaction of floating bridge pontoons and its effect on the bridge dynamic responses," Marine Structures, Vol. 83. https://doi.org/10.1016/j.marstruc.2022.103174.

[9] Liu, Z., Dai, C., Cui, X., Wang, Y., Liu, H., Zhou, B., 2024, "Hydrodynamic interactions between ships in a fleet," Journal of Marine Science and Engineering, Vol. 12(1): 56. https://doi.org/10.3390/jmse12010056.

[10] Dmitrieva, I. N., 1994, "Numerical Investigations of Hydrodynamic coefficients and Hydrodynamic Interaction between Two Floating Structures in Waves," Report No. 1018, Ship Hydrodynamic Laboratory, Delft University of Technology. http://resolver.tudelft.nl/uuid:dc2790c0-5304-45eb-9a8d-4c24a5569de0

[11] Kashiwagi, M., Endo, K. and Yamaguchi, H., 2005, "Wave Drift Forces and Moments on Two Ships arranged Side by Side in Waves," Ocean Engineering, 32, pp. 529-555. https://-doi.org/10.1016/j.oceaneng.2004.09.005.

[12] Ali, M. T., 2021, "A Numerical Investigation on Hydrodynamic Interaction Coefficients for a Group of Truncated Composite Cylinders Floating in Waves." 40th International Conference on Ocean, Offshore and Arctic Engineering, OMAE2021-63037. https://doi.org/10.1115/OMAE2021-63037.